

Synthesis and Characterization of Magnetite and Cobalt Ferrite Nanoparticles by Sol-Gel Auto Combustion Technique

S. D. Raut¹, S. G. Dahotre², L. N. Singh³, S. N. Jadhav⁴

¹ Research Scholar, ² Professor, Head, Department of Physics
Dr. Babasaheb Ambedkar Technological University, Lonere, Mangaon, Raigad, India, 402103,

Received on: 16 July, 2021

Revised on: 10 August, 2021

Published on: 12 August, 2021

Abstract- Magnetite and Cobalt ferrite nanoparticles were prepared by sol-gel auto combustion technique. This method is very simple and easy to achieve magnetite and cobalt ferrite nanoparticles in powder form. The nanocrystalline forms of synthesized sample were obtained at very low annealing temperature of about 600^o C. From XRD, it reveals that cobalt ferrite nanoparticles are highly crystalline in nature and average crystallite size obtained is almost 30nm. SEM image shows the cubic spinel form of synthesized sample. Vibrating sample magnetometer is used to study the magnetic properties which shows that the saturation magnetization of cobalt ferrite is higher than saturation magnetization of magnetite nanoparticles, also anisotropic constant of cobalt ferrite nanoparticles is higher than magnetite nanoparticles, confirms the single domain of sample which is also verified by squareness ratio. It is observed from FTIR characterization that, the metal-oxide bonds like Fe-O and Co-O are present in the sample. The obtained results of cobalt ferrite nanoparticles are having more advantageous than magnetite nanoparticles for the applications of MRI and magnetic sensors.

Keywords- Magnetite, Cobalt ferrite, Magnetic properties, sol-gel auto combustion.

I. INTRODUCTION

Complex oxides such as magnetite and cobalt ferrite are very interesting materials. Their structural, magnetic, optical and electrical properties help to improve the

applications of spintronics devices [1]. In recent years most promising technology is spintronics which introduce to reduce device size, speeding up processing data and store the information in small area [2][3]. In 1988 magnetite is introduced as half metal which gives single spin state either up or down. It gives more advantageous to store the information. This effective magnetic material is applied for spin based devices such as MRI, MRAM, gas sensor [3] [4][5][6]. To improve the magnetic properties for spintronics, here I have studied cobalt doped magnetite. Cobalt ferrite is selected due to high density and high magnetocrystalline anisotropy [7][8]. In this research magnetite (Fe₃O₄) is replaced by cobalt ferrite (CoFe₂O₄). Comparative study has been done for the study of structural and magnetic properties of magnetite and cobalt ferrite.

Different methods have been used to synthesize magnetite and cobalt ferrite such as co-precipitation, mechano-chemical, thermal hydrolysis, sol-gel, sol-gel auto combustion[9][10][11][12][13]. Among various methods sol gel auto combustion is very simple and requires less time for synthesis of sample.

II. LITERATURE REVIEW

V.R. bhagwat et. al., reported the synthesis of cobalt ferrite carried out by sol-gel auto combustion method

using three different fuels such as ethylene glycol, urea and glycine. From XRD crystalline size obtained in the range of 22.10 to 15.11 nm. It has been also observed that, saturation magnetization, remenant magnetization and coercivity increases with the increase in size of the the nanoparticles[14].

Thapa et. al. and co-workers reported in research work the crystalline size calculated is below 10 nm due to which surface effects cause saturation magnetization decreases and hence magnetite materials changes from ferromagnetic to superparamagnetic in nature which is used for flexible spintronics devices[15].

Hassan Soleimani, et. al., studied the cobalt substituted magnetite by co-precipitation method. The crystalline size calculated in the range 13 nm to 35 nm with increase in Co^{2+} ions concentration from XRD. It also observed the FTIR analysis of cobalt substituted magnetite which gives qualitative study of the ions at tetrahedral and octahedral sites was observed at wavenumbers ranging from 600 to 400 cm^{-1} . It has been observed from FTIR, presence of metal oxygen bond in the cobalt substitute magnetite [16].

III. METHODOLOGY

Chemicals

All Iron nitrate, cobalt Nitrate, deionized water, citric acid (AR grade), $[\text{NH}_4\text{OH}]$ ammonia solution to maintain pH were purchased from Merck and used without further purification.

Synthesis Method

Iron nitrate, cobalt nitrate and citric acid were used for the preparation of cobalt ferrite are of AR grade. A known quantity of Iron nitrate and cobalt nitrate was dissolved in deionized water and mixed with citric acid as 1:1 molar ratio. To maintain the pH 7, add ammonia solution drop wise. This solution was stirred for 2 hours and then a sol gets formed. The solution was then heated to 90⁰ C for 2 hours to form a brownish gel. This gel was decomposed at same temperature in oven. The gel then converted into fluffy powder consists of homogeneous flakes of very small particle size shown in Fig. 1. This powder was crushed by using mortar and pestle and placed for annealing in muffle furnace at temperature 600⁰ C gives fine powder of sample for characterization of XRD, FESEM, VSM and FTIR.



Fig.1 - Synthesized fluffy powder of cobalt ferrite

IV. RESULT & DISCUSSION

Characterizations

The nanoparticles were characterized with the help of XRD, FESEM, VSM and FTIR. The XRD measurement carried out using Cu-K α radiation. FESEM image carried out for study of surface morphology. VSM characterization gives information regarding magnetic properties at room temperature and FTIR spectra recorded in the range of 4000 cm^{-1} to 400 cm^{-1} .

X-ray Diffraction (XRD) study

Fig. 2 shows the XRD peaks which gives crystalline nature of magnetite and cobalt ferrite. The various peaks of magnetite at 30.30⁰, 35.65⁰, 43.56⁰, 54.08⁰, 57.59⁰ and 62.99⁰ are obtained and in cobalt ferrite various peaks obtained at 30.20⁰, 35.54⁰, 43.19⁰, 53.56⁰, 57.09⁰ and 62.76⁰. It reveals that the minor shift in peak position may happen due to ionic radius of Co^{2+} which is slightly greater than Fe^{2+} ion[17] [18].

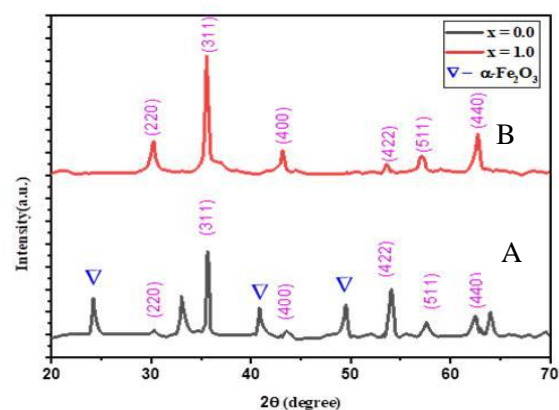


Fig.2 – XRD graph of magnetite and cobalt ferrite.

The XRD pattern of magnetite peak (A) shows that minor impurity of hematite ($\alpha\text{-Fe}_2\text{O}_3$) is present in sample and strong reflection of peaks are obtained at (220), (311), (400), (422), (511) and (440). From peak (B) it has been observed that no additional impurity is present. From the XRD graph both peak shows the FCC type of spinel structure[14].

We have calculated various parameters as lattice constant (a), x-ray density, volume of unit cell, hopping length at tetrahedral site (L_A), hopping length at octahedral site (L_B), and crystallite size from XRD graphs which are shown in Table 1.

Table 1: Various parameters of magnetite and cobalt ferrite

Parameters	Magnetite (Average)	Cobalt ferrite (Average)
Lattice constant (a)	8.3334 Å	8.3749 Å
Crystallite size(D)	34.02 nm	30.8 nm
X-ray density (ρ) (g/cc)	5.31355	5.307141
Unit cell volume(V)	578.7642Å ³	587.4145 Å ³
Hopping length (L_A)	3.608 Å	3.626 Å
Hopping length (L_B)	2.946 Å	2.960 Å

The average crystalline size (D) was calculated by using the Scherrer's formulae.

$$D = \frac{K\lambda}{\beta \sin \theta}$$

Where, K is crystallite constant (0.94), λ is wavelength, β is FWHM and θ is peak position.

From the above Table 1 it is observed that crystallite size of magnetite is 34.02 nm whereas for cobalt ferrite it is 30.8 nm. From this we conclude that when we add cobalt in pure magnetite, crystallite size decreases due to minor shift in peak position of synthesized sample which confirms that, crystallite size is dependent on M^{2+} ion . The hopping length is the distance between magnetic ions in the given sample. In pure magnetite and cobalt ferrite, tetrahedral and octahedral sites are present due to which lattice constant influences on hopping length [19]. From above, it concludes that the hopping length varies due to doping of cobalt in pure magnetite.

Field Emission Scanning Electron Microscopy (FESEM)

Fig. 3 and Fig.4 shows the FESEM images of magnetite and cobalt ferrite, which consist of random distribution of

agglomerated particles originated from the eruption of fuels during synthesis process.

The sponge like morphology is observed in cobalt ferrite sample.

Vibrating Sample Magnetometer(VSM)

The magnetic properties of magnetite and cobalt ferrite samples were recorded by using VSM at room temperature with applied field ranging upto 1500 Oe is shown in Fig.5 and Fig.6. The magnetic hysteresis loop confirms that the sample shows ferromagnetic performance with soft and hard magnetic nature of magnetite and cobalt ferrite sample [14].

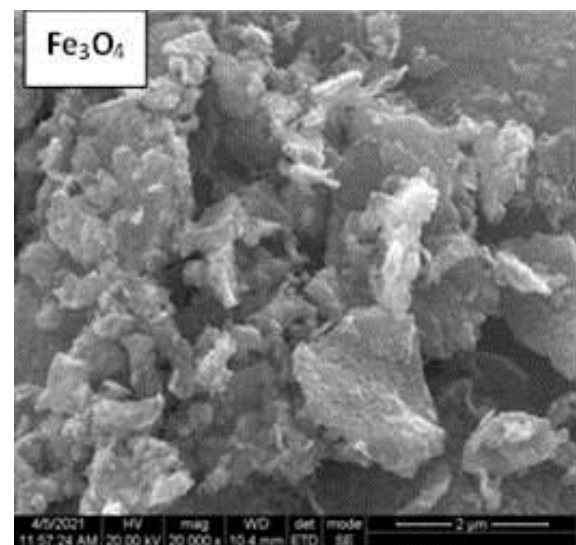


Fig.3 -FESEM image of magnetite sample

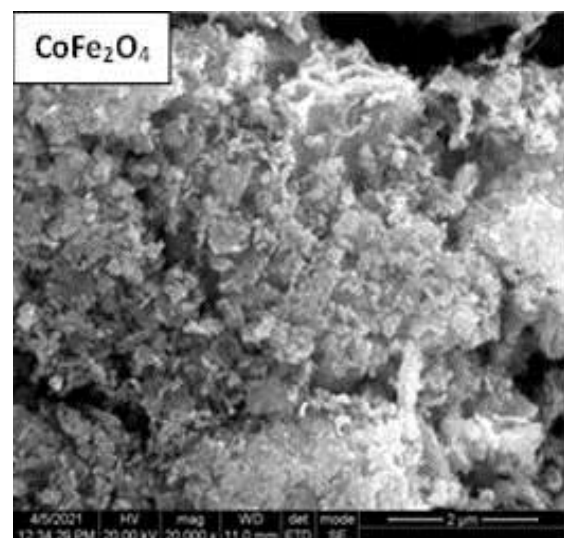


Fig.4 - FESEM image of Cobalt ferrite

Coercivity (H_c), remanence magnetization (M_r), saturation magnetization (M_s) and magnetic crystalline

anisotropy (K) values are summarized in Table 2.

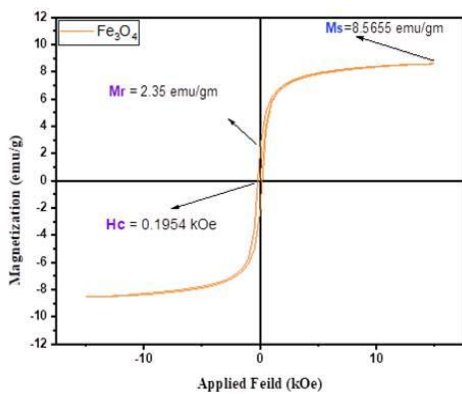


Fig.5 – VSM graph of pure magnetite

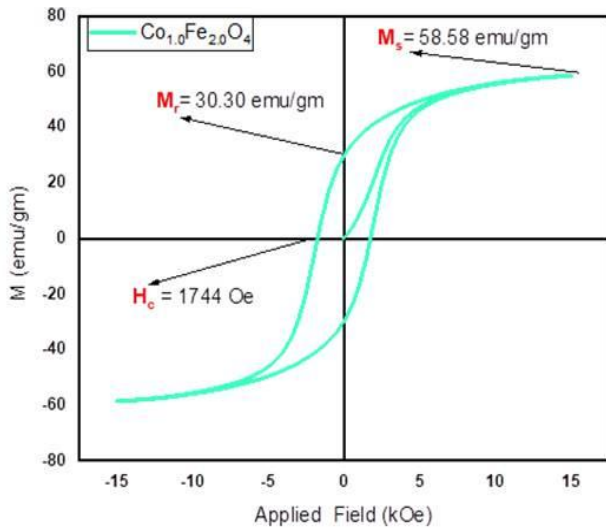


Fig.6 – VSM graph of cobalt ferrite

Table 2-Variou parameters of magnetic material

Parameters	Magnetite	Cobalt ferrite
Coercivity (Hc)	195.4 Oe	1744 Oe
Saturation magnetization (Ms)	8.565 emu/g	58.58 emu/g
Remanence Magnetization (Mr)	2.35 emu/g	30.30 emu/g
Squareness ratio (Mr/Ms)	0.27	0.51
Magnetocrystalline anisotropy (K)	1743.43615 erg/g	106420.333 erg/g

From Table 2, it concludes that saturation magnetization increases due to Co^{2+} ions. It may happen as ionic radii of Co^{2+} ions greater than Fe^{2+} ions. Since squareness ratio of cobalt ferrite is around 0.5 which indicates the single domain nature of the sample [20][21]. The Magnetocrystalline anisotropy (K) is also high which is

potential applications of spintronics.

Fourier Transformer Infra-Red Spectroscopy (FTIR)

The Fourier Transform Infra-red spectroscopy recorded for the synthesized sample of magnetite and cobalt ferrite shows the presence of metal oxygen bond. The various frequencies obtained are as shown in Table 3.

Table 3- FTIR data of magnetite and cobalt ferrite

sample	$\bar{\nu}_1$	$\bar{\nu}_2$	$\bar{\nu}_3$	$\bar{\nu}_4$
Pure magnetite	3444.1	1635.37	549.71	470.63
Cobalt ferrite	3429.4	1635.6	580.57	412.77

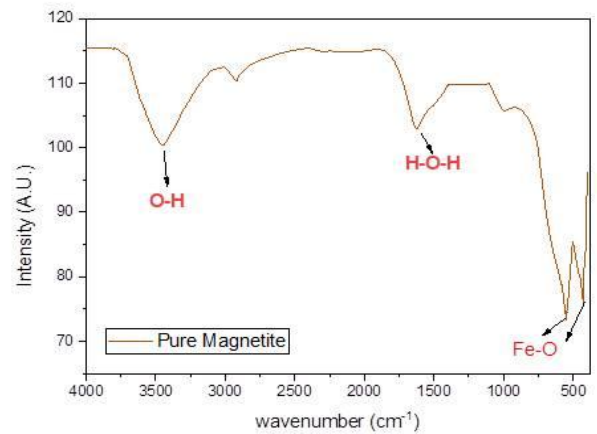


Fig.7 – FTIR spectrum of magnetite

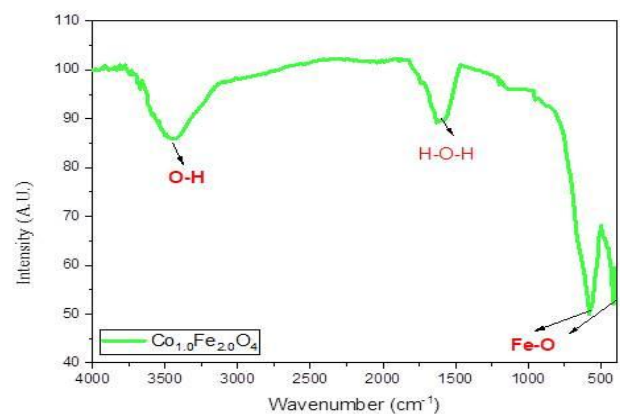


Fig. 8- FTIR spectrum of cobalt ferrite

The Fig. 7 and Fig. 8 shows the FTIR graph of pure magnetite and cobalt ferrite which helps to show various bonds present in synthesized sample. $\bar{\nu}_1 = 3444.1 \text{ cm}^{-1}$, 3429.4 cm^{-1} indicates the O-H bond in the functional group region. $\bar{\nu}_2 = 1635.37 \text{ cm}^{-1}$, 1635.6 cm^{-1} indicates the presence of H-O-H bond due to deionized water which is

used at the time of synthesis process [16]. \bar{v}_3 and \bar{v}_4 shows the Fe^{3+} -O bond at tetrahedral site and Fe^{2+} -O at octahedral site respectively. It shows maximum absorption of infra-red light due to metal and non-metal ion bonding.

V. CONCLUSION

Synthesis of pure magnetite and cobalt substituted magnetite is successfully carried out with sol-gel auto combustion method. Synthesized cobalt substituted magnetite is in the nanoscale range. Pure magnetite has slightly larger crystallite size than cobalt ferrite. The FESEM image shows the morphology of magnetite and cobalt ferrite and confirms spinel structure of sample. From VSM graph it concludes that, coercivity, saturation magnetization and magnetocrystalline anisotropy of cobalt ferrite is greater than that of pure magnetite which is potential applications of MRI, gas sensor, MRAM. From FTIR it is observed that metal-oxide (M-O) bond is present in the range of 580 cm^{-1} to 400 cm^{-1} . Due to higher intensity of peaks of cobalt ferrite, stretching and vibrations of Co-O bond is greater than that of Fe-O bond. Finally, it has been concluded that, cobalt doped magnetite is more effective than the pure magnetite.

ACKNOWLEDGMENT

Authors are thankful to the Dr. Sandesh Jaybhaye for XRD characterization facility. The authors also thankful to acknowledge SAIF, IIT madras for providing characterization facilities

REFERENCES

- [1] R. K. Kotmala and J. Shah, *Ferrite Materials: Nano to Spintronics Regime*, vol. 23. Elsevier, 2015.
- [2] S. Mesoraca, S. Knudde, D. C. Leitao, S. Cardoso, and M. G. Blamire, "All-spinel oxide Josephson junctions for high-efficiency spin filtering," 2018.
- [3] S. Bhatti, R. Sbiaa, A. Hirohata, H. Ohno, S. Fukami, and S. N. Piramanayagam, "Spintronics based random access memory: a review," *Mater. Today*, vol. 20, no. 9, pp. 530–548, 2017, doi: 10.1016/j.matod.2017.07.007.
- [4] T. A. Lastovina et al., "Solvothermal synthesis of Sm^{3+} doped Fe_3O_4 nanoparticles," *Mater. Sci. Eng. C*, vol. 80, pp. 110–116, 2017, doi: 10.1016/j.msec.2017.05.087.
- [5] N. M. Caffrey, D. Fritsch, T. Archer, S. Sanvito, and C. Ederer, "Spin-filtering efficiency of ferrimagnetic spinels CoFe_2O_4 and NiFe_2O_4 ," pp. 1–8, 2013.
- [6] W. Liu, P. K. J. Wong, and Y. Xu, "Hybrid spintronic materials: Growth, structure and properties," *Prog. Mater. Sci.*, vol. 99, no. February 2018, pp. 27–105, 2019, doi: 10.1016/j.pmatsci.2018.08.001.
- [7] B. J. Rani, M. Ravina, B. Saravanakumar, G. Ravi, V. Ganesh, and S. Ravichandran, "Nano-Structures & Nano-Objects Ferrimagnetism in cobalt ferrite (CoFe_2O_4) nanoparticles," vol. 14, pp. 84–91, 2018, doi: 10.1016/j.nanos.2018.01.012.
- [8] N. M. Caffrey, D. Fritsch, T. Archer, S. Sanvito, and C. Ederer, "Spin-filtering efficiency of ferrimagnetic spinels CoFe_2O_4 and NiFe_2O_4 ," *Phys. Rev. B - Condens. Matter Mater. Phys.*, vol. 87, no. 2, pp. 1–7, 2013, doi: 10.1103/PhysRevB.87.024419.
- [9] D. A. Rayan, M. A. Zayed, and G. M. A. Al Maqsood, "Structure , Optical , and Magnetic Properties of Magnetite Nanoparticles Doped with Zinc and Lanthanum and Prepared in Oxygen and Nitrogen Atmosphere," vol. 2, pp. 1–11, 2019, doi: 10.32371/jtmc/236083.
- [10] B. Kalska-Szostko, U. Wykowska, D. Satula, and P. Nordblad, "Thermal treatment of magnetite nanoparticles," *Beilstein J. Nanotechnol.*, vol. 6, no. 1, pp. 1385–1396, 2015, doi: 10.3762/bjnano.6.143.
- [11] T. Iwasaki et al., "Mechanochemical preparation of magnetite nanoparticles by coprecipitation," *Mater. Lett.*, vol. 62, no. 25, pp. 4155–4157, 2008, doi: 10.1016/j.matlet.2008.06.034.
- [12] A. B. Shinde, "Structural and Electrical Properties of Cobalt Ferrite Nanoparticles," no. 4, pp. 64–67, 2021.
- [13] R. S. Yadav et al., "Structural, Cation Distribution, and Magnetic Properties of CoFe_2O_4 Spinel Ferrite Nanoparticles Synthesized Using a Starch-Assisted Sol-Gel Auto-Combustion Method," *J. Supercond. Nov. Magn.*, vol. 28, no. 6, pp. 1851–1861, 2015, doi: 10.1007/s10948-015-2990-0.
- [14] V. Bhagwat, A. Humbe, ... S. M.-M. S. and, and undefined 2019, "Sol-gel auto combustion synthesis and characterizations of cobalt ferrite nanoparticles: different fuels approach," Elsevier, Accessed: Jul. 08, 2021. [Online]. Available: <https://www.sciencedirect.com/science/article/pii/S0921510719301916>.
- [15] D. Thapa, V. R. Palkar, M. B. Kurup, and S. K. Malik, "Properties of magnetite nanoparticles synthesized through a novel chemical route," *Materials Lett.*, vol. 58, pp. 2692–2694, 2004, doi: 10.1016/j.matlet.2004.03.045.
- [16] H. Soleimani, N. R. A. Latiff, H. M. Zaid, N. Yahya, A. R. Sadrolhosseini, and M. Adil, "Influence of cobalt substitution on the structural and magnetic properties of cobalt substituted magnetite," *AIP Conf. Proc.*, vol. 1787, 2016, doi: 10.1063/1.4968106.
- [17] S. Kanagesan, ... M. H.-D. J. of, and undefined 2013, "SOL-GEL AUTO-COMBUSTION SYNTHESIS OF COBALT FERRITE AND IT'S CYTOTOXICITY PROPERTIES.," search.ebscohost.com, vol. 20, no. 4, pp. 1601–1610, 2013, Accessed: Jul. 08, 2021. [Online]. Available: <http://search.ebscohost.com/login.aspx?direct=true&profile=ehost&scope=site&authtype=crawler&jrnl=18423582&AN=97593330&h=3Y42e3oTWzDEqtm%2B117rZEUSdXC7OtzY7YDHxciphePxlU7PTZ9yXYzHb4NPzchdFV17IbU%2Bk8tsiqH6mtKGUQ%3D%3D&crl=c>.
- [18] V. P. Senthil, J. Gajendiran, S. G. Raj, T. Shanmugavel, G. Ramesh Kumar, and C. Parthasaradhi Reddy, "Study of structural and magnetic properties of cobalt ferrite (CoFe_2O_4) nanostructures," *Chem. Phys. Lett.*, vol. 695, pp. 19–23, Mar. 2018, doi: 10.1016/j.cplett.2018.01.057.
- [19] S. Anjum and A. Masud, "Structural and temperature dependent dielectric properties of tin substituted cobalt ferrites ($\text{Sn}_x\text{Co}_{1-x}\text{Fe}_2\text{O}_4$)," *Dig. J. Nanomater. Biostructures*, vol. 13, no. 4, pp. 1063–1080, 2018.
- [20] L. Kumar, P. Kumar, A. Narayan, and M. Kar, "Rietveld analysis of XRD patterns of different sizes of

- nanocrystalline cobalt ferrite*," *Int. Nano Lett.*, vol. 3, no. 1, 2013, doi: 10.1186/2228-5326-3-8.
- [21] R. S. S. Aravazhi, C. Selva, and S. Senthil, "Tuning of ferrites - ($Co_x Fe_{3-x} O_4$) nanoparticles by co - precipitation technique," *SN Appl. Sci.*, vol. 1, no. 3, pp. 1–11, 2019, doi: 10.1007/s42452-019-0244-7.